

International Journal of Hydromechatronics

ISSN online: 2515-0472 - ISSN print: 2515-0464
<https://www.inderscience.com/ijhm>

3D profile-based pothole segmentation and quantification

Zhihao Pan, Jinchao Guan, Xu Yang, Anthony Guo, Xin Wang

DOI: [10.1504/IJHM.2023.10057576](https://doi.org/10.1504/IJHM.2023.10057576)

Article History:

Received:	11 March 2023
Last revised:	15 April 2023
Accepted:	19 April 2023
Published online:	11 January 2024

3D profile-based pothole segmentation and quantification

Zhihao Pan

School of Engineering,
Monash University Malaysia,
Jalan Lagoon Selatan, Bandar Sunway,
47500 Subang Jaya, Malaysia
Email: Zhihao.Pan@monash.edu

Jinchao Guan

School of Highway,
Chang'an University,
Middle-Section of Nan'er Huan Road, Xi'an,
710064 ShaanXi Province, China
Email: guan@chd.edu.cn

Xu Yang

College of Future Transportation,
Chang'an University,
Middle-Section of Nan'er Huan Road, Xi'an,
710064 ShaanXi Province, China
Email: yang.xu@chd.edu.cn

Anthony Guo and Xin Wang*

School of Engineering,
Monash University Malaysia,
Jalan Lagoon Selatan, Bandar Sunway,
47500 Subang Jaya, Malaysia
Email: anthony.guo@monash.edu
Email: wang.xin@monash.edu
*Corresponding author

Abstract: With the increasing traffic load, pavement distresses are caused inevitably. Water penetration and extreme weather condition speed up the deterioration of pavements and cause the occurrence of potholes. Automated pothole inspection methods have been developed with both 2D and 3D-based imaging techniques for many years. However, the performances suffer from either accuracy or efficiency. In this paper, a 3D profile-based solution is proposed to inspect potholes with high accuracy and efficiency. A low-cost stereo imaging system is deployed to generate the 3D pothole profile, and an algorithm integrating region growing is developed to segment potholes. The pothole volume is calculated based on the segmentation results and the depth

information. Overall, the proposed method outperforms the existing method by 1.72% and 5.192% in pothole segmentation and quantification, respectively. Moreover, the proposed method has no demand for large-scale datasets and training procedures, thus reducing time and labour costs.

Keywords: pothole segmentation, pothole quantification, stereo imaging, region growing.

Reference to this paper should be made as follows: Pan, Z., Guan, J., Yang, X., Guo, A. and Wang, X. (2024) '3D profile-based pothole segmentation and quantification', *Int. J. Hydromechatronics*, Vol. 7, No. 1, pp.16–30.

Biographical notes: Zhihao Pan received her Bachelor's degree from North University of China, China, in 2016 and Master's degrees from North University of China, China, and Warsaw University of Technology, Poland in 2019. She is currently a PhD student at School of Engineering, Monash University Malaysia. Her current research interests include pavement crack inspection using deep learning and 3D imaging, and path planning algorithms for automated pavement crack repair.

Jinchao Guan received his Bachelor's degree from Nanjing Tech University, China, in 2018. He is currently a PhD student at the School of Highway, Chang'an University. His current research interests include 3D digital reconstruction for transportation infrastructure, deep learning for pavement health monitoring, and mathematical optimisation for pavement maintenance planning.

Xu Yang received his Bachelor's degree from Southeast University, China, in 2009, and PhD degree from Michigan Technological University, USA, in 2015. He is currently a Professor at the College of Future Transportation, Chang'an University, China. He has published over 120 papers with more than 4,000 citations (Google Scholar) in peer reviewed journals and conference proceedings. His research interests include advanced road pavement construction and maintenance technology, deep learning for automated pavement distress detection, and numerical simulation for civil engineering materials.

Anthony Guo is a Professor in Mechanical Engineering, and the Head of School, for both the School of Engineering and the School of Information Technology at Monash University Malaysia. Prior to joining Monash in 2009, He developed his academic career at Nanyang Technological University, Singapore. He obtained his BEng from Nanjing University of Aeronautics and Astronautics, China, and his PhD from Imperial College London, UK. He has research interests in stress wave propagation, application of ultrasound, piezoelectric transducer, smart materials and structures, material characterisation, non-destructive testing techniques etc. He has published widely with over 130 publications in journals and conferences, secured competitive research grants over \$2 million.

Xin Wang is a senior member at IEEE and received her PhD degree from Nanyang Technological University (NTU), in 2007. She was a Research Fellow with the Robotics Research Centre, NTU, from 2007 to 2009. She was an Assistant Professor with the Faculty of Engineering and Science, Universiti Tunku Abdul Rahman, from 2009 to 2012. She is currently an Associate Professor with the School of Engineering, Monash University Malaysia. Her research interests include optical metrology, 3D imaging, non-destructive inspection, and machine vision.

1 Introduction

Among all the pavement diseases, pothole is one of the most common diseases that occurs in cold and rainy regions (Dong et al., 2014; Yang et al., 2017; Hafezzadeh et al., 2021). Potholes develop from a deteriorated area of pavement, and the penetration of water and freezing speed up the occurrence of potholes (Biswas et al., 2018). The growth of potholes brings hazard and risk to the traffic and the safety of society, making the immediate pothole inspection and repair indispensable. So far, most of potholes are reported and inspected manually, which leads to high labour cost and puts the inspectors at risk (Saad and Tahar, 2019). Therefore, automated pothole inspection methods are developed lately to assist related departments in assessing the condition and planning maintenance for pavement surfaces. The inspection of pothole can be conducted in two steps: pothole segmentation and pothole quantification. The segmentation of pothole produces a binary pothole map showing the location and the shape of the pothole. The generated binary pothole map can be further used in pothole quantification. The quantification calculates the geometrical information of the pothole which enables an assessment of the severity. Consequently, repair strategies can be determined, and the cost of repair can be estimated based on the volume of the pothole (Ravi et al., 2020).

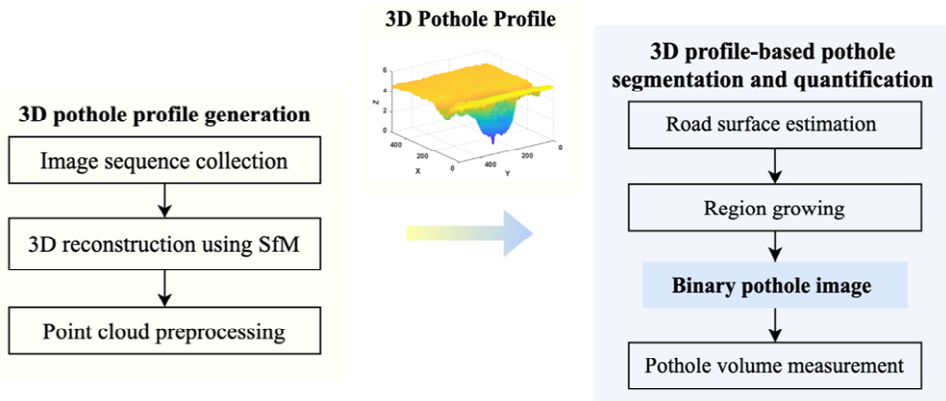
The development of computer vision facilitated the research in 2D imaging-based pothole detection and segmentation. Traditional image processing-based methods were first developed to segment potholes from the images captured by digital cameras. Pattern recognition was applied to extract the low-level features of the pothole using hand-crafted representation (Koch and Brilakis, 2011; Tedeschi and Benedetto, 2017; Radopoulou and Brilakis, 2017). Edge detection-based methods were proposed to segment potholes by analysing the greyscale distribution of the pothole images (Nienaber et al., 2015; Akagic et al., 2017; Wang et al., 2017). Furthermore, support vector machine (SVM) was deployed in machine learning-based methods to differentiate the texture feature between potholes and pavement surface (Lin and Liu, 2010; Gao et al., 2020). However, all the methods mentioned above are predisposed to surrounding noises, such as uneven illumination, water stains, and so on. With the advance of deep learning, convolution neural networks (CNNs) significantly improve the precision of pothole detection and segmentation in overcoming the problem of background noise (Pan et al., 2018; Sathvik et al., 2022; Feng et al., 2022b; Ranyal et al., 2023). Nonetheless, the training of CNNs requires large-scale datasets, which is highly time and labour consuming, detracting the efficiency and practicality of CNNs.

Except for 2D imaging-based methods, 3D-based methods were developed to acquire the 3D geometrical information of potholes. Low-cost sensor systems were developed with Microsoft Kinect to detect and measure the geometrical parameters of the potholes (Joubert et al., 2011; Moazzam et al., 2013; Jahanshahi et al., 2013), but the accuracy is limited by the illumination condition (Mathavan et al., 2015). To increase the accuracy, mobile laser system was widely used to obtain the detail information of the road surface and detect pavement distresses from the reconstructed point cloud (van der Horst et al., 2019; De Blasiis et al., 2020). Feng et al. (2022a) segmented the pothole from the point cloud reconstructed using mobile laser system. Then the detected potholes were quantified from depth, area, and diameter. Even though laser-based systems provide promising performance, cost of the system is generally expensive. Lately, the advances in stereo imaging system make the reconstruction of 3D scenes more accessible, and structure from motion (SfM) is the most popular method. SfM reconstructs the 3D model

from a series of images without knowing the position of the cameras (Ullman, 1979). Saad et al. (2019) collected the image sequences from different altitudes using unmanned aerial vehicle (UAV) and evaluated the impact of altitude on the precision of pothole detection. Tan and Li (2019) reconstructed the 3D pavement model from the UAV-collected image sequences and quantified the pothole from width, length, height, and area. Roberts et al. (2020) developed a low-cost stereo imaging system which collected image sequences using mobile phones. Guan et al. (2021) proposed a GoPro-equipped stereo imaging system to obtain the depth information of the pothole, and the collected depth information was incorporated to train a U-Net-based neural network for pothole segmentation. Then the pothole volume was calculated based on the generated binary pothole map. Except the methods mentioned above, 3D ground-penetrating radar (GPR) was also applied to diagnose pavement and detect pavement distresses (Fontul et al., 2021; Liang et al., 2022). Though the above literatures proposed various methods to segment and quantify potholes, they suffer from either low accuracy or efficiency.

In this paper, we propose a 3D profile-based solution to segment and quantify potholes efficiently and accurately. A low-cost GoPro-equipped stereo imaging system is deployed to collect image sequences of potholes from multiple perspectives. SfM is applied to reconstruct the 3D pothole point cloud model, and point cloud preprocessing is implemented to generate the 3D pothole profile. An algorithm integrating road surface estimation and region growing is developed based on the 3D profile to segment the pothole and produce the binary pothole image. Eventually, the pothole volume is calculated using the binary pothole image and depth information. The overview of the proposed method is shown in Figure 1. The results demonstrate that the proposed method improves the existing method in both accuracy and efficiency.

Figure 1 Overview of the proposed 3D profile-based pothole segmentation and quantification (see online version for colours)



2 3D pothole profile generation

2.1 Data collection

To obtain the 3D pothole point cloud model accurately and efficiently, a GoPro-equipped stereo imaging system was deployed to capture high-resolution image sequences of potholes from multiple perspectives. Figure 2 illustrates the layout of the deployed stereo imaging system. Three GoPro cameras are mounted on the rear of the vehicle and distributed with a space of 0.6m horizontally for large field-of-view and high reconstruction accuracy. The distance between the cameras and the pavement surface is 0.8m vertically. The central camera is mounted to be perpendicular to the pavement surface, while the other two cameras on the side are inclined to the centre with 30 degrees. With the above settings, 2m² of road surface can be captured with a ground sampling distance (GSD) of 0.27 mm/pix. Besides, an overlap rate of 70%~80% can be guaranteed to produce high-quality details of the road surface (Saad and Tahar, 2019). More parameter settings of the GoPro cameras can be found in Table 1. The cameras are controlled with a remote to capture pothole images simultaneously and continuously while the vehicle is moving. To avoid system vibration and motion blur, the vehicle moves with a speed of 3–15 km/h.

Figure 2 GoPro-equipped stereo imaging systems (see online version for colours)



Table 1 Parameter settings of the GoPro cameras

<i>Parameters</i>	<i>Properties</i>
Image size	4,000 × 3,000 pixels
Pixel size	1.5 μm × 1.5 μm
ISO range	100–1600
Frame rate	2–10 FPS
Lens mode	Linear
Focal length	27mm

2.2 3D reconstructions

SfM is applied to reconstruct the 3D pothole point cloud model. Without knowing the position of the target and cameras, SfM reconstructs the 3D point cloud model from the

overlapping images. Firstly, key points are extracted and matched among image pairs. Then the relative pose between two cameras is calculated using the extracted key points based on the theory of epipolar geometry. Consequently, spatial coordinates of the captured points are derived from the geometric correlation between the images and space. In our research, the captured pothole image sequences are split into batches with the size of 20-30 images and fed into PhotoScan to compile the dense point cloud. Based on our previous study (Guan et al., 2021), the implemented stereo imaging system reconstructs the 3D pothole point cloud model with an absolute accuracy at millimetre level. An average relative error of 5.40% was verified by comparing the manual measurement of the pothole depth and the 3D measurement obtained from the reconstructed point cloud model.

2.3 Point cloud preprocessing

Since the orientation of the compiled point cloud model is random, calibration is first conducted to rotate the reconstructed pavement surface onto the X-Y plane using principal component analysis (PCA). PCA estimates the three principal directions of the model, which are represented by the three eigenvectors of the point cloud. The eigenvector with the minimum eigenvalue denotes the normal vector of the point cloud. By multiplying the coordinates of points with the normal vector, the original point cloud is geometrically rotated to the X-Y plane.

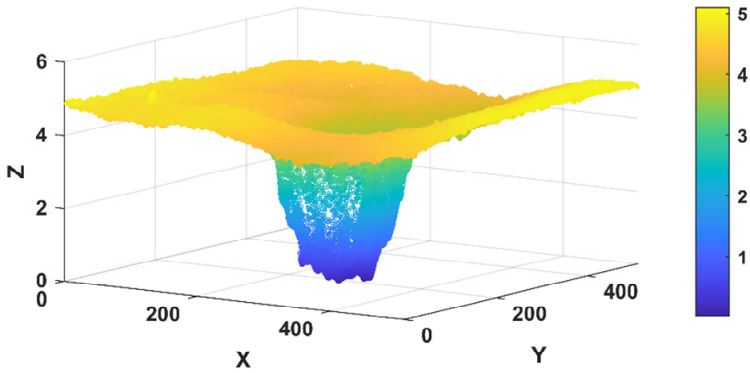
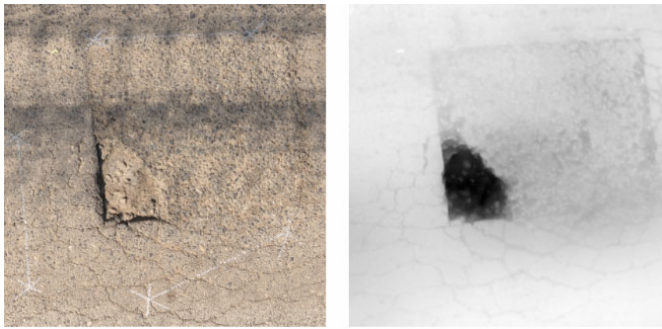
Furthermore, the points in the point cloud model generated by SfM cannot be indexed orderly. To facilitate further calculation, we vectorise the dense point cloud to generate an $M \times N$ point cloud array. The dense point cloud is split into spaces along X and Y-axis with a certain step calculated as

$$step = \frac{\max(x) - \min(x)}{M} \quad (1)$$

in which, $\max(x)$ and $\min(x)$ are the maximum and minimum value of X in the dense point cloud, M is the number of rows in the point cloud array, and 512 is used in this study. Then the number of columns of the point cloud array can be determined as

$$N = \frac{\max(y) - \min(y)}{step} \quad (2)$$

in which $\max(y)$ and $\min(y)$ are the maximum and minimum value of Y in the dense point cloud. After vectorisation, the points in the point cloud array can be indexed as (m, n, d) , where $m \in [0, M)$, $n \in [0, N)$. The value of d represents the depth of the point, which is calculated by averaging the depth of all the points inside each split space. In the end, the 3D profile of the captured pothole is represented by the vectorised point cloud array. Figure 3 shows an example of the generated 3D pothole profile. Besides, RGB and depth orthoimages are generated to visualise the pothole as shown in Figure 4. The RGB orthoimage is obtained by taking the average RGB value of the points in each split space, while the greyscale of the pixel (m, n) in the depth orthoimage is the value of d .

Figure 3 An example of the generated 3D pothole profile (see online version for colours)**Figure 4** (a) RGB orthoimage (b) Depth orthoimage

3 3D profile-based pothole segmentation and quantification

This section introduces the proposed 3D profile-based pothole segmentation and quantification method. Based on the generated 3D pothole profile, a plane is first fitted to simulate the pavement surface. Then region growing algorithm is implemented to segment the pothole from the pavement surface and generate the binary pothole image. With the segmentation result and depth information provided by the 3D pothole profile, the volume of the pothole is calculated.

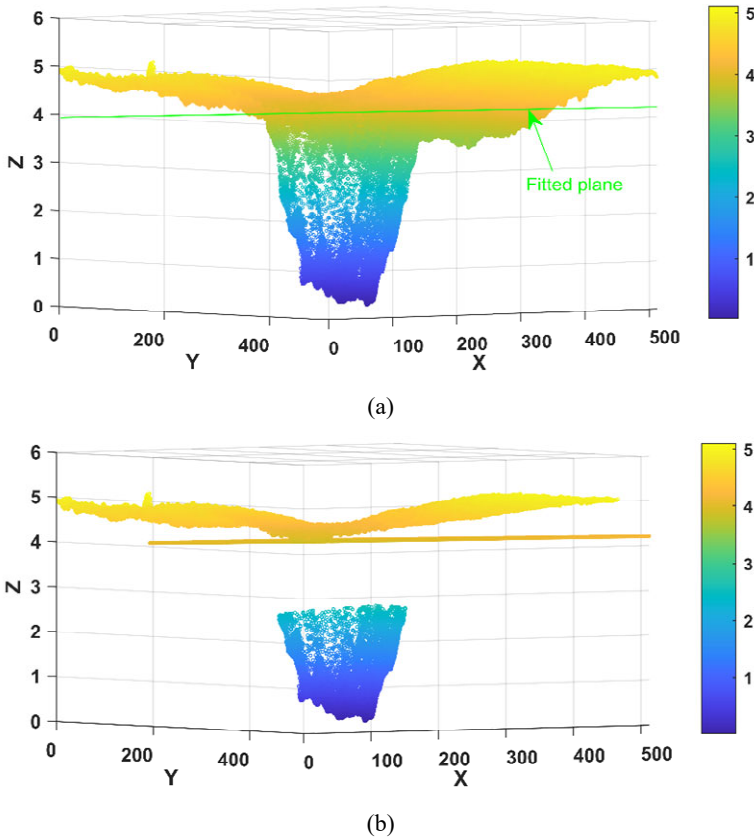
3.1 Pothole segmentation

3.1.1 Pavement surface estimation

According to Figure 3, the points belonging to the pavement surface and the points inside the pothole can be differentiated from altitude. Compared with the pothole, the points on the pavement surface present more consistent altitude. Therefore, a plane that represents the pavement surface can be fitted. In this study, 3-dimensional random sample consensus (RANSAC) is implemented to fit the plane. RANSAC predicts the mathematical model without considering outliers (Fischler and Bolles, 1981).

Presumably, a given dataset is comprised of inliers and outliers, RANSAC iteratively chooses elements from the given dataset to estimate the mathematical model until a satisfied model is obtained. The pavement surface estimated using RANSAC is plotted in Figure 5(a), showing that most of points inside the pothole locate below the estimated pavement surface. However, except for the pothole, noisy points caused by pavement unevenness also distribute under the fitted plane. To reduce the impact of pavement unevenness, we fit all the inliers of the fitted plane to the plane itself. The inliers mentioned here are the points that are selected as inliers when implementing RANSAC. The result after reducing pavement unevenness is given in Figure 5(b).

Figure 5 Results of pavement surface estimation, (a) result of estimating pavement surface using RANSAC (b) result after reducing pavement unevenness (see online version for colours)



3.1.2 Region growing

According to Figure 5(b), the pothole can be segmented from the pavement surface by selecting all the points below the estimated plane. However, there are chances that noisy points still exist below the plane even after reducing the pavement unevenness. Therefore, instead of simply selecting the points below the estimated plane, region growing is applied for pothole segmentation. In region growing algorithm, an initial seed

is first determined, then the region grows by iteratively including the neighbours of the seed that satisfy the pre-defined criterion (Adams and Bischof, 1994). In our case, the algorithm is implemented based on the vertical distance between the point and the estimated pavement surface. As shown in Figure 5(b), if we grow the region from the lowest point, the boundary of the pothole can be determined when the examined point reaches the estimated plane. Hence, the distance D between the examined point and the estimated plane can be used as the criterion that stops the region growing. Given an estimated pavement surface $ax + by + cz = e$ and an examined point (x_i, y_i, z_i) , the distance $D(x_i, y_i, z_i)$ is calculated as

$$D(x_i, y_i, z_i) = \frac{|ax_i + by_i + cz_i|}{\sqrt{a^2 + b^2 + c^2}}. \quad (3)$$

Overall, in the implemented region growing algorithm, we determine the lowest point in the 3D pothole profile as the initial seed. The criterion used to stop the region growing is when $D(x_i, y_i, z_i) < 10^{-4}$, and 4-connected neighbours of the seed are examined.

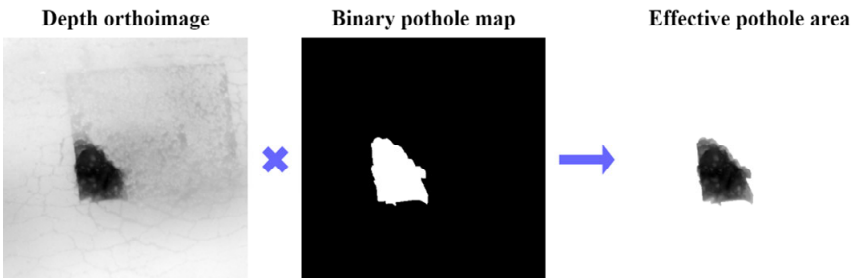
3.2 Pothole quantification

The knowledge of volume enables an estimation for the material cost spent in pothole repair (Wang et al., 2022). Thus, we quantify the pothole by measuring the volume in this study. The volume of a pothole is calculated based on the area and depth of the pothole. With the segmented binary pothole image, the location of the pothole can be determined, meaning that the effective area for volume measurement can be extracted. By overlapping the binary pothole image with the depth orthoimage, the depth of each pixel in the pothole region can be obtained. Figure 6 shows an example of effective pothole area extraction. Based on the extracted area, the volume of every single pixel can be calculated by multiplying the area and the depth of the pixel. Consequently, the pothole volume is acquired by accumulating the volume of all the pixels. The calculation is given as below:

$$Volume = S \cdot \sum_k^K d_k \quad (4)$$

where K is the number of pixels of the segmented pothole region, S is the area of the pixel, d_k is the depth of the k^{th} pixel.

Figure 6 The extraction of effective pothole area for volume calculation (see online version for colours)



4 Results

This section discusses the results of the proposed 3D profile-based pothole segmentation and quantification method. Six potholes are studied to evaluate the performance of the proposed method. Moreover, the deep learning-based pothole segmentation method proposed by Guan et al. (2021) is compared.

4.1 Pothole segmentation

Figure 7 and Table 1 list the qualitative and quantitative results of comparing the proposed pothole segmentation method against the deep learning-based method proposed by Guan et al. (2021). The ground-truth images were obtained by manually labelling the RGB orthoimages. To quantitatively evaluate the segmentation results, intersection over union (IoU) between the ground-truth A and the predicted binary pothole map B is calculated. IoU is a metric that quantifies the overlap between the ground-truth and segmentation result. The value of IoU is calculated as follows:

$$IoU(A, B) = \frac{A \cap B}{A \cup B}, \quad (5)$$

where $A \cap B$ is the overlap area of A and B , and $A \cup B$ combines the area of A and B . Therefore, the value of IoU is penalised not only when the overlap area is low, but also when the segmentation result overflows the ground-truth.

According to quantitative comparison given in Table 1, the proposed method outperforms Guan's method by 1.72% in IoU. Qualitatively, the proposed method segments the pothole with more boundary details. The lack of detailed boundary information in deep learning-based method can be introduced from two perspectives. On the one hand, the ground-truth images used for training the neural network are not labelled properly. It can be noticed from the RGB orthoimages that the boundary of pothole is hardly to be identified by human eyes due to the pavement texture and the surrounding pavement diseases, thus increasing the difficulty of manual labelling. On the other hand, the unpredictable shape of potholes increases the requirement of the diversity of the dataset. Due to the lack of diversified dataset, the neural network is trained to predict certain patterns instead of differentiating the features of pothole and background. Therefore, a large-scale and diversified dataset is essential for training neural networks that segment potholes with high precision. However, the establishment of such dataset is highly time and labour-consuming. On the contrary, the proposed method segments potholes by extracting and processing the 3D pothole geometrical information, thus having no demand for dataset and training procedure. Overall, the proposed method segments potholes with higher accuracy and lower time and labour cost compared with deep learning-based methods.

Figure 7 Qualitative comparison results of pothole segmentation, (a) 3D pothole profile (b) RGB orthoimage (c) ground-truth images (d) Guan et al. (2021) (e) proposed method (see online version for colours)

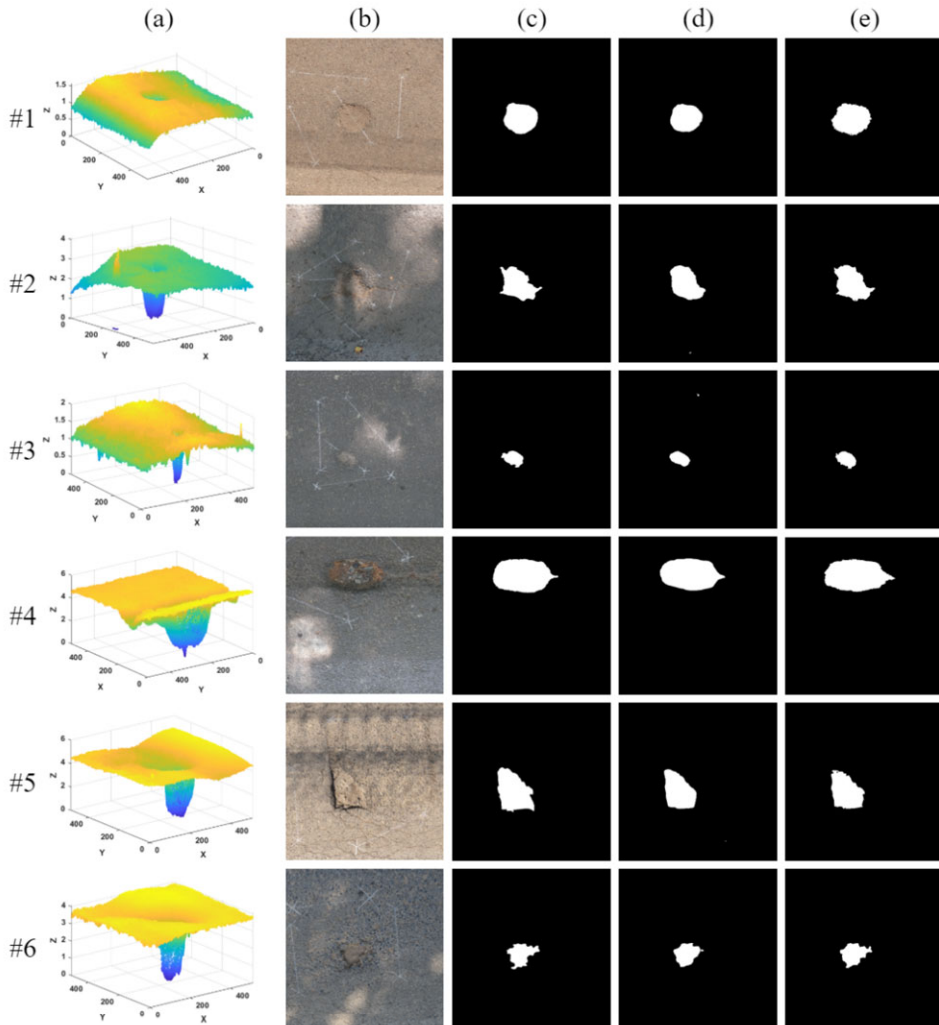


Table 1 Quantitative comparison results of pothole segmentation

<i>Pothole no.</i>	<i>IoU</i>	
	<i>Guan et al. (2021)</i>	<i>Proposed method</i>
#1	0.8377	0.8465
#2	0.8106	0.8548
#3	0.8171	0.8134
#4	0.8781	0.8827
#5	0.8025	0.8104
#6	0.8093	0.8510
Mean IoU	0.8259	0.8431

4.2 Pothole quantification

Figure 8 shows the extracted effective area for pothole volume calculation of the proposed method, and Table 2 compares the volume measurement results against Guan et al. (2021) and manual measurement. The manual measurement of the pothole volume was measured using sand replacement method. The volume measurement results of Guan et al. (2021) were obtained based on the binary pothole images shown in Figure 7(d). According to Table 2, the most and least severe potholes are Pothole #4 and Pothole #3 since they provide the highest and lowest volume, respectively. Based on the effective area given in Figure 8, even though Pothole #1 is larger than Pothole #5 and #6, the volume of Pothole #1 is the lowest among the three potholes, meaning that Pothole #5 and #6 are deeper than Pothole #1. Generally, both methods underestimate the pothole volume, but the proposed method produces the results that are closer to the manual measurement. Overall, the relative error of the proposed method is 5.192% lower than the method proposed by Guan et al. (2021). Since the volume is calculated based on the area of the extracted pothole, the accuracy of volume measurement is directly affected by the performance of pothole segmentation. Therefore, the outperformance in pothole volume measurement also proves our superiority in pothole segmentation.

Figure 8 The results of extracting effective area for pothole volume calculation, (a) depth orthoimages (b) the extracted effective areas

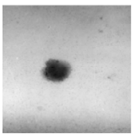
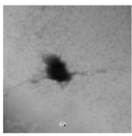
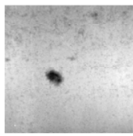
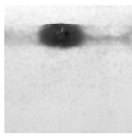
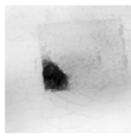
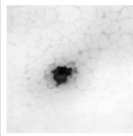
	Pothole #1	Pothole #2	Pothole #3	Pothole #4	Pothole #5	Pothole #6
(a)						
(b)						
Area (pixels)	9622	9125	2428	17353	9597	4743

Table 2 The comparison results of pothole volume calculation

Pothole no.	Volume/cm ³			Relative error (%)	
	Manual measurement	Guan et al. (2021)	Proposed method	Guan et al. (2021)	Proposed method
#1	366	301	349	17.760	4.645
#2	1088	1029	1087	5.423	0.092
#3	139	114	123	17.986	11.511
#4	2520	2422	2541	3.889	0.833
#5	1536	1559	1563	1.497	1.758
#6	669	601	624	10.164	6.726
Mean relative error (%)				9.453	4.261

5 Conclusions

In this paper, we propose a 3D profile-based pothole segmentation and quantification method. A GoPro-equipped stereo imaging system is deployed to reconstruct the 3D point cloud model of the pothole, and preprocessing is implemented to generate the 3D pothole profile. An algorithm integrating region growing is developed to differentiate the pothole from the pavement surface and generate the binary pothole image. The pothole volume is then calculated based on the effective area extracted from the binary pothole image. According to the quantitative comparison results, the proposed method outperforms the existing deep learning-based method by 1.72% and 5.192% in pothole segmentation and quantification, respectively. Moreover, the proposed method has no demand for dataset and training procedures which are highly time and labour consuming. Hence, the proposed method improves the existing method in both accuracy and efficiency. For future work, we will work on quantifying potholes from more perspectives, such as width and diameter, to facilitate the severity assessment of potholes.

Acknowledgements

This study is supported by the Smart Manufacturing Research Node, Monash University.

References

- Adams, R. and Bischof, L. (1994) ‘Seeded region growing’, *IEEE Transactions on Pattern Analysis and Machine Intelligence*, Vol. 16, No. 6, pp.641–647.
- Akagic, A., Buza, E. and Omanovic, S. (2017) ‘Pothole detection: An efficient vision based method using RGB color space image segmentation’, in *2017 40th International Convention on Information and Communication Technology, Electronics and Microelectronics (MIPRO)*, pp.1104–1109.
- Biswas, S., Hashemian, L. and Bayat, A. (2018) ‘Investigation of pothole severity and maintenance methods in Canada through questionnaire survey’, *Journal of Cold Regions Engineering*, Vol. 32, No. 2, p.04018002.
- De Blasiis, M.R., Di Benedetto, A. and Fiani, M. (2020) ‘Mobile laser scanning data for the evaluation of pavement surface distress’, *Remote Sensing*, Vol. 12, No. 6, p.942.
- Dong, Q., Huang, B. and Zhao, S. (2014) ‘Field and laboratory evaluation of winter season pavement pothole patching materials’, *International Journal of Pavement Engineering*, Vol. 15, No. 4, pp.279–289.
- Feng, Z., El Issaoui, A., Lehtomäki, M., Ingman, M., Kaartinen, H., Kukko, A., Savela, J., Hyypä, H. and Hyypä, J. (2022a) ‘Pavement distress detection using terrestrial laser scanning point clouds – accuracy evaluation and algorithm comparison’, *ISPRS Open Journal of Photogrammetry and Remote Sensing*, Vol. 3, p.100010.
- Feng, Z., Guo, Y., Liang, Q., Bhutta, M.U.M., Wang, H., Liu, M. and Sun, Y. (2022b) ‘MAFNet: segmentation of road potholes with multimodal attention fusion network for autonomous vehicles’, *IEEE Transactions on Instrumentation and Measurement*, Vol. 71, pp.1–12.
- Fischler, M.A. and Bolles, R.C. (1981) ‘Random sample consensus: a paradigm for model fitting with applications to image analysis and automated cartography’, *Commun. ACM*, Vol. 24, No. 6, pp.381–395.
- Fontul, S., Solla, M. and Pérez-Gracia, V. (2021) ‘Flexible pavement diagnosis methodology based on GPR assessment’, in *2021 11th International Workshop on Advanced Ground Penetrating Radar (IWAGPR)*, pp.1–6.

- Gao, M., Wang, X., Zhu, S. and Guan, P. (2020) 'Detection and segmentation of cement concrete pavement pothole based on image processing technology', *Mathematical Problems in Engineering*, Vol. 2020, p.1360832.
- Guan, J., Yang, X., Ding, L., Cheng, X., Lee, V.C.S. and Jin, C. (2021) 'Automated pixel-level pavement distress detection based on stereo vision and deep learning', *Automation in Construction*, Vol. 129, p.103788.
- Hafezzadeh, R., Autelitano, F. and Giuliani, F. (2021) 'Asphalt-based cold patches for repairing road potholes – an overview', *Construction and Building Materials*, Vol. 306, p.124870.
- Jahanshahi, M.R., Jazizadeh, F., Masri, S.F. and Becerik-Gerber, B. (2013) 'Unsupervised approach for autonomous pavement-defect detection and quantification using an inexpensive depth sensor', *Journal of Computing in Civil Engineering*, Vol. 27, No. 6, pp.743–754.
- Joubert, D.A., Tyatyantsi, A., Mphahlehle, J. and Manchidi (2011) 'Pothole tagging system', in *4th Robotics and Mechatronics Conference of South Africa (RobMech 2011)*, pp.23–25.
- Koch, C. and Brilakis, I. (2011) 'Pothole detection in asphalt pavement images', *Advanced Engineering Informatics*, Vol. 25, No. 3, pp.507–515.
- Liang, X., Yu, X., Chen, C., Jin, Y. and Huang, J. (2022) 'Automatic classification of pavement distress using 3d ground-penetrating radar and deep convolutional neural network', *IEEE Transactions on Intelligent Transportation Systems*, Vol. 23, No. 11, pp.22269–22277.
- Lin, J. and Liu, Y. (2010) 'Potholes detection based on SVM in the pavement distress image', in *2010 Ninth International Symposium on Distributed Computing and Applications to Business, Engineering and Science*, pp.544–547.
- Mathavan, S., Kamal, K. and Rahman, M. (2015) 'A review of three-dimensional imaging technologies for pavement distress detection and measurements', *IEEE Transactions on Intelligent Transportation Systems*, Vol. 16, No. 5, pp.2353–2362.
- Moazzam, I., Kamal, K., Mathavan, S., Usman, S. and Rahman, M. (2013) 'Metrology and visualization of potholes using the microsoft kinect sensor', in *16th International IEEE Conference on Intelligent Transportation Systems (ITSC 2013)*, pp.1284–1291.
- Nienaber, S., Booysen, M.J. and Kroon, R.S. (2015) 'Detecting potholes using simple image processing techniques and real-world footage', in *34th Annual Southern African Transport Conference (SATC 2015)*, pp.153–164.
- Pan, Y., Zhang, X., Cervone, G. and Yang, L. (2018) 'Detection of asphalt pavement potholes and cracks based on the unmanned aerial vehicle multispectral imagery', *IEEE Journal of Selected Topics in Applied Earth Observations and Remote Sensing*, Vol. 11, No. 10, pp.3701–3712.
- Radopoulou, S.C. and Brilakis, I. (2017) 'Automated detection of multiple pavement defects', *Journal of Computing in Civil Engineering*, Vol. 31, No. 2, p.04016057.
- Ranyal, E., Sadhu, A. and Jain, K. (2023) 'Automated pothole condition assessment in pavement using photogrammetry-assisted convolutional neural network', *International Journal of Pavement Engineering*, Vol. 24, No. 1, p.2183401.
- Ravi, R., Habib, A. and Bullock, D. (2020) 'Pothole mapping and patching quantity estimates using LiDAR-based mobile mapping systems', *Transportation Research Record*, Vol. 2674, No. 9, pp.124–134.
- Roberts, R., Inzerillo, L. and Di Mino, G. (2020) 'Exploiting low-cost 3D imagery for the purposes of detecting and analyzing pavement distresses', *Infrastructures*, Vol. 5, No. 1, p.6.
- Saad, A.M. and Tahar, K.N. (2019) 'Identification of rut and pothole by using multirotor unmanned aerial vehicle (UAV)', *Measurement*, Vol. 137, pp.647–654.
- Sathvik, M., Saranya, G. and Karpagaselvi, S. (2022) 'An intelligent convolutional neural network based potholes detection using Yolo-V7', in *2022 International Conference on Automation, Computing and Renewable Systems (ICACRS)*, pp.813–819.
- Tan, Y. and Li, Y. (2019) 'UAV photogrammetry-based 3D road distress detection', *ISPRS International Journal of Geo-Information*, Vol. 8, No. 9, p.409.

- Tedeschi, A. and Benedetto, F. (2017) 'A real-time automatic pavement crack and pothole recognition system for mobile Android-based devices', *Advanced Engineering Informatics*, Vol. 32, pp.11–25.
- Ullman, S. (1979) 'The interpretation of structure from motion', *Proceedings of the Royal Society of London. Series B, Biological Sciences*, Vol. 203, No. 1153, pp.405–426.
- Van Der Horst, B.B., Lindenbergh, R.C. and Puister, S.W.J. (2019) 'Mobile laser scan data for road surface damage detection', *Int. Arch. Photogramm. Remote Sens. Spatial Inf. Sci. XLII-2/W13*, pp.1141–1148.
- Wang, P., Hu, Y., Dai, Y. and Tian, M. (2017) 'Asphalt pavement pothole detection and segmentation based on wavelet energy field', *Mathematical Problems in Engineering*, Vol. 2017, p.1604130.
- Wang, T., Dra, Y.A.S.S., Cai, X., Cheng, Z., Zhang, D., Lin, Y. and Yu, H. (2022) 'Advanced cold patching materials (CPMs) for asphalt pavement pothole rehabilitation: state of the art', *Journal of Cleaner Production*, Vol. 366, p.133001.
- Yang, X., You, Z., Hiller, J. and Watkins, D. (2017) 'Correlation analysis between temperature indices and flexible pavement distress predictions using mechanistic-empirical design', *Journal of Cold Regions Engineering*, Vol. 31, No. 4, p.04017009.